Incorporating Physical-Layer Effects in Modeling of MAC Protocols Operating in MANETs

Hui Xu, J.J. Garcia-Luna-Aceves [‡]
xuhui, jj@soe.ucsc.edu
[‡]Computer Engineering Department
University of California, Santa Cruz
Santa Cruz, CA 95064, USA

Hamid R. Sadjadpour [†]
hamid@soe.ucsc.edu
[†]Electrical Engineering Department
University of California, Santa Cruz
Santa Cruz, CA 95064, USA

***Abstract*—We present an analytical framework for the performance evaluation of medium access control (MAC) protocols with and without carrier sensing operating in mobile ad hoc networks (MANETs). The model captures the functionality of MAC protocols together with the characterization of packet reception under a realistic physical layer that impacts the performance of the MAC protocols due to interference caused by concurrent transmissions, channel fading caused by multi-path effect, and node mobility. The model reveals the interplay between the MAC protocol functionality and network parameters, and provides new insight on the performance of MAC protocols operating in multi-hop wireless networks. The analytical results are corroborated with results obtained using discrete-event simulations.**

I. Introduction

While the impact of physical (PHY) layer behaviors on the performance of MANETs is well recognized, it has been largely ignored in analytical models for the sake of simplicity in the study of medium access control (MAC) protocols operating in multi-hop wireless networks (e.g., see [1], [2]). Previous analytical models basically use a common collision model in which an ideal physical layer is assumed in that a packet transmission/reception is assumed to succeed if there are no other concurrent transmissions.

However, the success of a packet reception is related to the signal to interference plus noise ratio (SINR), and the packet can be only successfully received with some probability [3] at the physical layer, which is mainly due to two factors. First, because of multi-path and channel fading (caused by node movement) effects, the signal power from one transmission varies and becomes a function of space and time [4]. Secondly, different MAC protocols deal with concurrent transmission attempts differently, which causes the effect of interference signals vary also [5]. Network parameters, such as network size and node mobility, determine the node-to-node distance, which is a crucial factor for quantifying signal power; both network traffic intensity and the logic of MAC protocols impact the node transmission probability; the type of channel fading and concurrent interference signals also impact the SINR.

Some prior work has tried to incorporate physical-layer effects in the modeling of MAC protocols, while avoiding a precise characterization of the physical layer for the sake of simplicity. For example, Zheng et al. [6] approximated the effect of imperfect channel conditions based on an assumption that bits are transmitted with a fixed error probability; Carvalho et al. [5] used linear approximations for the relationship among probabilities of the channel being busy, a node transmitting, and a packet being received successfully.

A few works have attempted to analyze the behavior of the physical layer and incorporate the net effect in the modeling of MAC protocols. For example, Pham et al. [7], [8] have tried to characterize imperfect channel conditions based on a specific Rayleigh fading channel, while still using a collision model rather than a packet reception model that depends on the SINR; hence, those factors that determine the SINR values, which of course impact the packet reception probability, are not involved in their modeling.

In this paper, we take into account both fading channels and multiple access interference (MAI), and propose a parameterized framework that can represent the interaction between the physical (PHY) and MAC layers. The focus in this work is to provide a way for modeling MAC protocols with physical-layer behavior analysis. To show that, we study two basic types of MAC protocols, with and without carrier sensing where MAI is explicitly analyzed. We take two well known example protocols for each type, namely Aloha [9] and IEEE 802.11 DCF [10], and verify the correctness and accuracy of our model via simulations.

The rest of this paper is organized as follows. Section II presents our characterization of MAC protocols without carrier sensing (Aloha) and with carrier sensing (802.11 DCF) as Markov chains. Section III presents our characterization of a fairly realistic PHY layer in the context of a MANET, and derive the packet reception probability, which is used in the MAC model. Section IV continues the characterization of the PHY layer and derives the channel-busy probability for MAC protocols based on carrier sensing schemes. Section V derives the throughput of MAC protocols based on the formulations

[1]This work was partially sponsored by the U.S. Army Research Office under grants W911NF-04-1-0224 and W911NF-05-1-0246, by the National Science Foundation under grant CCF-0729230, by DARPA through Air Force Research Laboratory (AFRL) Contract FA8750-07-C-0169, and by the Baskin Chair of Computer Engineering. The views and conclusions contained in this document are those of the authors and should not be interpreted as representing the official policies, either expressed or implied, of the Defense Advanced Research Projects Agency or the U.S. Government.

derived in Sections III and IV for the values of probabilities for transmission, channel busy, and success packet reception. Section VI compares our analytical results against extensive Qualnet simulations based on various network scenarios, and Section VII concludes this paper.

II. Modeling MAC Protocols

We consider two representative MAC schemes, IEEE 802.11 DCF [10] and Aloha, for protocols with and without efficient interference prevention scheme, respectively.

A. Aloha

In the pure Aloha protocol [9] a node transmits packets immediately, without any carrier sensing or coordination with other nodes, and slotted Aloha [11] improves the utilization of the shared channel by synchronizing transmissions of devices within time-slots. If an ACK is not received within a time interval, the transmitter assumes that the frame has experienced a transmission failure, and then backs off with a random timer for a retransmission for this frame.

We propose a Markov chain model for the Aloha protocol with a random and independent backoff scheme. Let p denote the probability of packet transmission/reception failure for any node, and let $s(t)$ represent the stochastic retransmission stage $[0, M-1]$ at a time period from t to $t+1$. For each failed transmission, a node backs off with a random timer and the timer value $W_i (i \in [0, M-2])$ lies in the interval $[1, W]$, where W is the maximum window size. When the timer reaches zero, it enters the next retransmission stage. Let $b(t)$ denote the stochastic process representing the backoff time counter. Then, the process $[s(t), b(t)]$ can be modeled as the discrete-time Markov chain depicted in Fig. 1.

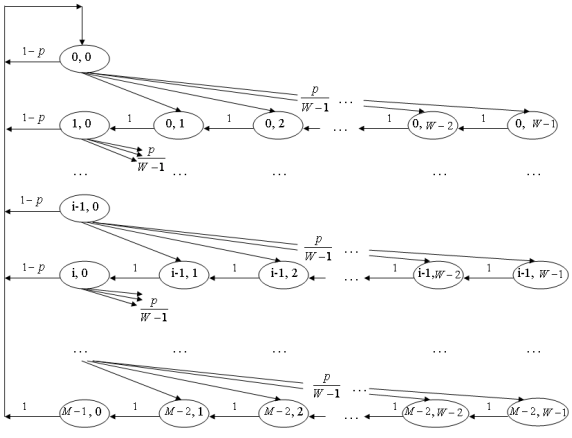

Fig. 1. Markov chain for Aloha protocol

Let $b_{i,k} = \lim_{t\to\infty} P\{s(t) = i, b(t) = k\}, i \in [0, M-1], k \in [0, W-1]$ represent the stationary state distribution of the Markov chain; the only non-null one-step transition probabilities are

$$\begin{array}{lll} P\{i,k|i,0\} = \frac{p}{W-1}, & k \in [1, W-1], & i \in [0, M-2] \\ P\{0,k|i,k\} = 1-p, & k = 0, & i \in [0, M-2] \\ P\{0,k|i,k\} = 1, & k = 0, & i = M-1 \\ P\{i,k-1|i,k\} = 1, & k \in [2, W-1], & i \in [0, M-2] \\ P\{i+1,0|i,k\} = 1, & k = 1, & i \in [0, M-2]. \end{array} \quad (1)$$

From Eq. 1 note that

$$\begin{array}{l} b_{i,1} = b_{i+1,0} \; and \; b_{i,0} \times p = b_{i,1}, \; i \in [0, M-2] \\ \Rightarrow b_{i+1,0} = b_{i,0} \times p \Rightarrow b_{i+1,0} = b_{0,0} \times p^{i+1}. \end{array} \quad (2)$$

In addition, we also note that

$$\begin{array}{l} b_{i,W-k} = b_{i,0}\frac{kp}{W-1}, \; i \in [0, M-2], k \in [1, W-1] \\ \Rightarrow b_{i,k} = b_{i,0}\frac{(W-k)p}{W-1} = b_{0,0}\frac{(W-k)p^{i+1}}{W-1}. \end{array} \quad (3)$$

From Eq. 3, we see that all values of $b_{i,k}$ in that figure can be expressed as functions of $b_{0,0}$. Then, according to the normalization condition,

$$\begin{array}{l} b_{0,0}(1 + \sum_{i=1}^{M-1} p^i + \sum_{i=0}^{M-2}\sum_{k=1}^{W-1}\frac{(W-k)p^{i+1}}{W-1}) = 1 \\ \Rightarrow b_{0,0}(1 + \frac{p(1-p^{M-1})}{1-p} + \frac{Wp(1-p^{M-1})}{2(1-p)}) = 1 \\ \Rightarrow b_{0,0}\frac{2+Wp-(W+2)p^M}{2(1-p)} = 1, \end{array} \quad (4)$$

we can obtain $b_{0,0} = \frac{2(1-p)}{2+Wp-(W+2)p^M}$. Let τ denote the transmission probability, then by taking $\tau = \sum_{i=0}^{M-1} b_{i,0}$, we obtain a function of p, the packet reception failure probability,

$$\tau = b_{0,0}\sum_{i=0}^{M-1} p^i = \frac{2(1-p^M)}{2+Wp-(W+2)p^M}. \quad (5)$$

B. IEEE 802.11 DCF

In the IEEE 802.11 DCF scheme, a node first senses the medium before transmitting a frame. After the medium is sensed idle for a time interval (a distributed interframe space, i.e., DIFS), the node starts to transmit. Otherwise, it defers transmission with a random backoff timer with a uniformly distributed value in $[0, CW]$, where CW stands for contention window and is initially set to its minimum value CW_{min}, and doubled after each time the frame incurs a transmission failure and schedules a retransmission, up to its maximum value CW_{max}. The backoff timer is suspended whenever the channel becomes busy, and reactivated after the channel is sensed idle again for a DIFS and decremented by one for each physical slot time. The node transmits when its backoff timer reaches zero. After the transmission, the transmitter expects to receive a positive acknowledgement (ACK) frame from the receiver within a time interval of Short InterFrame Space (SIFS). If an ACK is not received within a SIFS, the transmitter assumes that the frame has experienced a transmission failure, and then schedules a retransmission for this frame.

Carvalho et al. [5] modeled the IEEE 802.11 DCF and derived the following transmission probability of a node (τ) as a function of the packet transmission/reception failure probability (p) and the channel-busy probability (g):

$$\tau = \frac{2(1-g)(1-p^{M+1})(1-2p)}{(1-g^{M+1})(1-2p)(1-2g)+kW}, \quad (6)$$

where $W = CW_{min}$, M denotes the maximum retransmission number, m is the retransmission counter, and $k = (1-p_j)[1-(2p_j)^{M+1}]$ if $m = M$ and $k = 1-p_j\{1+(2p_j)^m[1+p_j^{M-m}(1-2p_j)]\}$ if $m < M$.

Given that p and g in Eq. 5 and 6 for τ are still unknown, we will analyze realistic PHY layer behaviors to derive them in the next two sections.

III. Modeling the PHY Packet Reception

A. Packet Reception

In the demodulation of each signal assuming a spread-spectrum system, signals from other nodes transmitting simultaneously over other channels appear as interference. Let Y denote the finite set of nodes spanning the network under consideration. The success of receiving a signal transmitted by a node i to a node w at the PHY layer is invariably related to the signal-to-interference-plus-noise ratio $SINR_i^w$ at node w [5], which is given by:

$$SINR_i^w = \frac{Q_i^w C_i}{\sum_{j \neq i,w}^{j \in Y} \chi_j Q_j^w + \delta_w^2}, \tag{7}$$

where Q_i^w represents the received power at node w from node i, Q_j^w denotes the interference power from j, C_i is the spreading gain of the spread-spectrum system, δ_w^2 is the background or thermal noise power at w, and χ_j is an on/off indicator with transmission probability τ of any node j, i.e., $\chi_j = 1$ if j transmits at the same time as node i, and $\chi_j = 0$ otherwise.

For a given SINR value, two signal (or packet) reception models are commonly used [12]. In the SINR-threshold (SINRT)-based model, the threshold value is denoted by β, and the SINR value is directly compared with β, and a signal or packet can be accepted only when the SINR value is above β, i.e., $SINR \geq \beta$. In the error-rate-threshold (ERT)-based model, the error rate threshold value is denoted by α, and the bit or packet error rate (BER/PER) is a function of the SINR value and the modulation scheme used, i.e., $BER/PER = F(SINR)$. A signal or packet can be successfully received only when the BER/PER value is below α, that is, $F(SINR) \leq \alpha \Rightarrow SINR \leq F^{-1}(\alpha)$, i.e., the ERT based scheme can be transformed to the SINRT based scheme with $\beta = F^{-1}(\alpha)$.

A packet can be successfully received when

$$\begin{aligned} SINR_i^w &= \frac{Q_i^w C_i}{\sum_{j \neq i,w}^{j \in Y} \chi_j Q_j^w + \delta_w^2} \geq \beta \\ &\Rightarrow \quad Q_i^w \geq \frac{\beta}{C_i}\Big(\sum_{j \neq i,w}^{j \in Y} \chi_j Q_j^w + \delta_w^2\Big). \end{aligned} \tag{8}$$

Therefore, the received power from the transmitter is required to be larger than a *reception power threshold* of RX_{th}, which can be defined as

$$RX_{th} = \frac{\beta}{C_i}\Big(\sum_{j \neq i,w}^{j \in Y} \chi_j Q_j^w + \delta_w^2\Big). \tag{9}$$

B. Channel-State Model for Packet Reception

1) The Representation of Fading Channels: Because of channel fading in MANETs, the received power Q_j^w by a node j from a node w is a continuous random variable with an area mean power $\overline{Q_j^w(d)}$, where d is the distance between the two nodes. Previous work [4] provides the probability density function (pdf) of the channel amplitude $r \geq 0$, $f_r(r)$, for all kinds of fading channels. For example, the Ricean fading pdf can be written as $f_r(r) = \frac{r}{\sigma^2} exp(-\frac{r^2 + r_s^2}{2\sigma^2}) I_0(\frac{r r_s}{\sigma^2})$, where r_s is the amplitude of the LOS signal, $I_0(\cdot)$ is the zeroth-order modified Bessel function of the first kind, the ratio $K = \frac{r_s^2}{2\sigma^2}$ is the Ricean factor, and $\sigma^2 = \overline{Q_r(d)}/(1+K)$. Note that $\overline{Q_r(d)}$ is the area mean power and can be calculated as $\overline{Q_r(d)} = Q_s/d^{\varepsilon}$, where Q_s denotes the transmission power used by a transmitter, and ε is the path loss exponent. Rayleigh fading [3] can be regarded as a special case when $K = 0$, that is, $f_r(r) = \frac{r}{\sigma^2} exp(-\frac{r^2}{2\sigma^2})$, where $\sigma^2 = \overline{Q_r(d)}$.

Because the signal power q is a function of the channel amplitude r as $q = \frac{r^2}{2}$, we can derive the pdf of any instantaneous received power Q_j^w as

$$f_q(q) = \frac{d(F_r(\sqrt{2q}) - F_r(-\sqrt{2q}))}{dq} = \frac{f_r(\sqrt{2q})}{\sqrt{2q}}, \tag{10}$$

and it is also a function of the node-to-node distance d.

2) Node-to-Node Distance Distribution in Mobile Networks: Since the inter-nodal distance d is a crucial factor in deriving the received power at any receiver. However, node mobility in MANETs causes node-to-node distance to vary, and a node-to-node distance distribution must be used.

Much work has been reported on the topology properties of MANETs with various mobility models. For example, Christian Bettstetter [13] studied random waypoint mobility model and derived the pdf of node-to-node distance d in a disk area with radius a, as $f_d(d) = \frac{1}{a} f_{\hat{d}}(\frac{d}{a})$, where

$$\begin{aligned} f_{\hat{d}}(\hat{d}) \quad = \quad & \frac{\hat{d}}{9\pi}[(6q^2 + (36\hat{d}^2 - 12)q - 36\hat{d}^2 + 24)\pi + \\ & (-12q^2 + (-72\hat{d}^2 + 24)q + 72\hat{d}^2 - 48)\arcsin\frac{\hat{d}}{2} \\ & + ((-\hat{d}^5 + 7\hat{d}^3 - 15\hat{d})q^2 + (2\hat{d}^5 - 23\hat{d}^3 - 6\hat{d})q \\ & - \hat{d}^5 + 16\hat{d}^3 + 12\hat{d})\sqrt{4 - \hat{d}^2}] \end{aligned} \tag{11}$$

with $\hat{d} = \frac{d}{a}$ and $q = \frac{E\{T_p\}}{E\{T_p\} + E\{T_m\}}$, where $E\{T_m\}$ denotes the expected movement time between two waypoints with $E\{T_m\} = \frac{0.905a}{V}$ for constant speed V, and T_p is pause time.

We assume that, the node-to-node distance distribution has been derived in previous work and is therefore a available for us to use.

3) Two-state Markov Chain Model: When channel fading does not change too fast within a time interval T, it can be approximated as a constant for a given packet transmission, while it may vary between different packet transmissions. That is, a packet may or may not be successfully received due to fading. Accordingly, a channel condition could be divided into "good" and "bad" states.

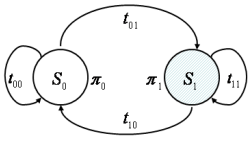

Fig. 2. Two state Markovian channel model

Let S denote an ordered finite set (*state space*) composed of states S_0 and S_1. Each state is sampled for one packet transmission period T under a given network scenario. S_0

represents the "bad" channel condition when the channel signal power is less than RX_{th}, i.e., the signal cannot be successfully received; S_1 presents the "good" channel condition when the power is larger than RX_{th}, i.e., the signal can be successfully received. That is, the instantaneous fading power $q(t) = r^2(t)/2$ is quantized with respect to a set of thresholds $B_0 = 0$, $B_1 = RX_{th}$ and $B_2 = +\infty$ as follows: *channel lies in S_k state if* $q(t) \in [B_k, B_{k+1})$ with $k = 0, 1$.

Babich et al. [14] have demonstrated that the quantized model can be approximated by a first-order Markovian model with the assumption of slow fading. Therefore, our Markovian channel state model can be as shown in Fig. 2 and the steady-state probability π_k can then be formulated as Eq. 12

$$\pi_k = P_r(\sqrt{2B_k} \le r \le \sqrt{2B_{k+1}}) = \int_{\sqrt{2B_k}}^{\sqrt{2B_{k+1}}} f(r)d_r. \quad (12)$$

The transition probabilities can be calculated from

$$\begin{array}{ll} t_{k,k+1} \approx \frac{N_{k+1}T}{\pi_k}, & k = 0 \\ t_{k,k-1} \approx \frac{N_kT}{\pi_k}, & k = 1 \\ t_{k,k} \approx 1 - \sum_{j=0,j\neq k}^{1} t_{k,j}, & k = 0, 1 \end{array} \quad (13)$$

where N_k is the average crossing rate of the instantaneous fading power through level B_k. The expression for N_k is

$$\begin{aligned} N_k &= f_D\sigma\sqrt{\pi}p(\sqrt{2B_k}) \\ &= f_D\sqrt{\frac{2\pi(1+K)B_k}{\varrho}}e^{-K}I_0(2\sqrt{\frac{K(1+K)B_k}{\varrho}}) \\ &\quad \times exp(-\frac{1+K}{\varrho}B_k) \end{aligned} \quad (14)$$

according to previous work [15], where $\varrho = \sigma^2 + \frac{1}{2}r_s^2$ is the local-mean fading power, $f_D = v/\lambda$ is the maximum Doppler shift, v is the mobile speed, and λ is the carrier wavelength.

C. Probability of Packet Reception

Based on our two-state Markov chain model for the wireless channel, when the channel is in "good" state, a packet can be successfully received, i.e., the packet transmission/reception success probability P_s is the steady-state probability of S_1; when channel is in "bad" state, a packet reception fails, i.e., the failure probability of P_f is the state probability of S_0, i.e.,

$$\begin{cases} P_s = \pi_1 = P_r(\sqrt{2RX_{th}} \le r \le \infty) = \int_{\sqrt{2RX_{th}}}^{\infty} f_r(r)d_r \\ P_f = \pi_0 = 1 - P_s. \end{cases} \quad (15)$$

Note that the channel amplitude pdf $f_r(r)$ is a function of the node-to-node distance d. For the performance evaluation, the expected probabilities with all possible values of d in certain network configuration are needed, that is,

$$\begin{cases} E[P_s] = \int_0^{\infty} P_s(d)f_d(d)d_d \\ E[P_f] = \int_0^{\infty} P_f(d)f_d(d)d_d, \end{cases} \quad (16)$$

where the $f_d(d)$ for networks with different configurations is also different and a sample is shown in Eq. 11.

Note that RX_{th}, defined in Eq. 9, is determined by the interference power, noise, and SINRT. The SINRT is a network parameter and noise is normally modeled as a white Gaussian process. Then, the only remaining factor to consider is the interference power. Because the slow fading channel state is sampled within a packet transmission interval T, the interference can be approximated by a constant during that period. That is, for a given network scenario during a transmission interval T, the RX_{th} has a given value.

D. Interference Model

Let $I_i^w = \sum_{j\neq i,w}^{j\in Y} \chi_j Q_j^w$ represent the sum of all interference power when node w is receiving packets from node i, where χ_j is the transmission on/off indicator with transmission probability of τ.

1) For MAC without Interference Prevention: In MAC protocols without carrier sensing such as Aloha, the transmission of any node j is only dependent on itself and is independent of other transmissions, i.e., χ_j can be assumed to be an independent variable. Therefore, the pdf of I_i^w, $f_{I_i^w}(q)$, produced by all the possible interference nodes can be expressed as an $n-2$ convolution (excluding the receiver w and transmitter i),

$$\begin{aligned} f_{I_i^w}(q) &= f_1^w \otimes \cdots \otimes f_{i-1}^w \otimes f_{i+1}^w \otimes \cdots \\ &\quad \otimes f_{w-1}^w \otimes f_{w+1}^w \otimes \cdots \otimes f_n^w(q), \end{aligned} \quad (17)$$

where $f_j^w(q)$ is the pdf of interference effect ($\chi_j Q_j^w$) caused by any interference node j, and n is the number of nodes in the network.

When node j transmits with probability τ, $\chi_j Q_j^w = Q_j^w$ and the pdf of interference power Q_j^w, denoted by $f_{Q_j^w}(q)$, can be calculated using Eq. 10. When node j does not transmit with probability $1-\tau$, $\chi_j Q_j^w = 0$, i.e., the interference power it causes equals zero. Therefore, if $\eta_q(Q_j^w)$ is used to denote a Dirac pulse at $q = Q_j^w$ and $\eta_q(0)$ is a Dirac pulse with $q = 0$, $f_j^w(q)$ can be formulated as

$$f_j^w(q) = \eta_q(0)(1-\tau) + \eta_q(Q_j^w)\tau. \quad (18)$$

Theoretically, $f_{I_i^w}(q)$ can be computed using Eq. 17. To be practical, consider any possible interfering node j with distance d_j to the receiver w, and let us focus on computing its average interference power over all the possible values of d_j, denoted by $E[Q_j^w]$. Given the pdf of the node-to-node distance $f_{d_j}(d_j)$ and the pdf of the instantaneous received power $f_q(q)$ shown in Eq. 10, we have

$$E[Q_j^w] = \int_0^{\infty}\int_0^{\infty} f_q(q(d_j))f_{d_j}(d_j)d_{d_j}d_q. \quad (19)$$

Eq. 18, the pdf of interference effect ($\chi_j Q_j^w$), can then be approximated as

$$f_j^w(q) \approx \eta_q(0)(1-\tau) + \eta_q(E[Q_j^w])\tau. \quad (20)$$

Then, Eq. 17 is approximated as an $n-2$ dimensional convolution for the function $f_j^w(q)$. To be more practical, we can even reduce the number of possible interfering nodes (also the convolution dimension) from $n-2$ to the number of nodes within perception range R_s. For example, suppose that the network is a disk area of radius a, $\left\lceil n \times \frac{\pi R_s^2}{\pi a^2} \right\rceil = \left\lceil \frac{nR_s^2}{a^2} \right\rceil$.

2) For MAC with Interference Prevention: In MAC without interference prevention, each node transmits independently; therefore, every other node could cause interference and the number of interference may be very large. In contrast, when interference prevention scheme (e.g. carrier sensing) is used as in IEEE 802.11 DCF, a node first senses the channel and transmits only if it determines that there are no other ongoing transmissions. Hence, the transmission of any node j is not

only dependent on itself but is also affected by its neighbors, which, in turn, depend on their neighbors' neighbors and so on. This is called the "cascade effect" and involves all network nodes. However, for practical purposes, transmission decisions can be considered independent if two nodes are sufficiently distant from each other (e.g., more than two hops away). That is, we can approximate a node's transmission behavior as being affected only by neighbor nodes within its two-hop perception range ($2R_s$). Let m represent the number of nodes in that area, then $m = \left\lceil n \times \frac{\pi(2\times R_s)^2}{\pi a^2} \right\rceil = \left\lceil \frac{4nR_s^2}{a^2} \right\rceil$, where a is the radius of network disk.

We note that Carvalho et al. [5] exploit the fact that MAI can be restricted within a certain bound (i.e., the number of interference for a transmission is limited) in the characterization of MAC protocols with interference prevention. They assumed that the probability of two concurrent transmissions in this area could be approximated as zero. However, in practical scenarios, there are no protocols that can prevent interference perfectly. Therefore, to be more accurate, in this paper we consider three different events: (a) there is no transmission at a given time (e_0), (b) there is one transmission (e_1), and (c) there are only two transmissions at a given time (e_2). Then we can investigate the probability of successful packet reception when interference exists.

Let A_j represent the event that a node j is transmitting, then the probability of event e_0 that "there is no ongoing transmission in an area with m nodes," denoted as $P\{e_0\}$, can be formulated as $P\{e_0\} = P\{\bigcap_{j=1}^{m} \overline{A_j}\} = 1 - P\{\bigcup_{j=1}^{m} A_j\}$, where $P\{\bigcup_{j=1}^{m} A_j\} = \sum_{j=1}^{m} P\{A_j\} - \sum_{j,k} P\{A_j \bigcap A_k\} + \sum_{j,k,l} P\{A_j \bigcap A_k \bigcap A_l\} + \cdots + (-1)^{m-1} P\{\bigcap_{j=1}^{m} A_j\}$. Because we assume that the probability of more than two concurrent transmissions can be approximated as zero, $P\{e_0\}$ can then be approximated by $P\{e_0\} \approx 1 - \sum_{j=1}^{m} P\{A_j\} + \sum_{j,k} P\{A_j \bigcap A_k\}$.

Now, we consider the event e_1 that "just one node transmits," and that node can be any one of m nodes. For the sake of argument, let us assume that node 1 is the node and the probability of e_1, $P\{e_1\}$, can then be formulated as $P\{e_1\} = mP\{\bigcap_{j=2}^{m} \overline{A_j} \bigcap A_1\} = mP\{\bigcap_{j=2}^{m} \overline{A_j} | A_1\} P\{A_1\} = m\{1 - P\{\bigcup_{j=2}^{m} A_j | A_1\}\} P\{A_1\}$, where according to our assumption $P\{\bigcup_{j=2}^{m} A_j | A_1\} \approx \sum_{j=2}^{m} P\{A_j | A_1\}$, $P\{e_1\}$ can then be approximated as $P\{e_1\} \approx m\{1 - P\{\sum_{j=2}^{m} A_j | A_1\}\} P\{A_1\} = m\{P\{A_1\} - \sum_{j=2}^{m} P\{A_j \bigcap A_1\}\}$.

Given that we approximate the probability of more than two concurrent transmissions as zero, the probability of event e_2 that "there are only two transmissions ongoing in an area with m nodes", denoted as $P\{e_2\}$, can then be calculated as $P\{e_2\} \approx 1 - P\{e_0\} - P\{e_1\}$.

Note that in the probability analysis for event e_1, we randomly pick node 1 as the transmitting node for the sake of argument; however, it can be any node. Therefore, let τ represent the transmission probability of any node, and then the probabilities of those three events can be derived as

$$\begin{aligned} P\{e_0\} &\approx 1 - m\tau + C_2^m \tau^2 (1-\tau)^{m-2}, \\ P\{e_1\} &\approx m\{\tau - (m-1)\tau^2\}, \\ P\{e_2\} &\approx m(m-1)\tau^2 - C_2^m \tau^2 (1-\tau)^{m-2}. \end{aligned} \quad (21)$$

Now let us come back to our interference analysis, where we assume that node i is transmitting to w with transmission probability τ. According to our assumption there will be no or only one interference. The probability of event e_{i0} that "there is no interference, i.e., only node i transmitting" is $P\{e_{i0}\} = P\{e_1\}/m = \tau - (m-1)\tau^2$. The probability of event e_{i1} that "there is one interfering node, i.e., only node i and another node are transmitting" is $P\{e_{i1}\} = P\{e_2\}/m = (m-1)\tau^2 - (m-1)\tau^2(1-\tau)^{m-2}/2 = (m-1)\tau^2(1-(1-\tau)^{m-2}/2)$.

When event e_{i0} occurs, the interference power equals zero; when event e_{i1} occurs, there is only one interference caused by a node j with a distance d_j to the receiver w, and the average interference power over all the possible values of d_j, denoted by $E[Q_j^w]$, has been shown in Eq. 19. Therefore, if $\eta_q(E[Q_j^w])$ is used to denote a Dirac pulse at $q = E[Q_j^w]$, and $\eta_q(0)$ is a Dirac pulse with $q = 0$, $f_{I_i^w}(q)$ can then be formulated as

$$\begin{aligned} f_{I_i^w}(q) &= \eta_q(0) P\{e_{i0}\} + \eta_q(E[Q_j^w]) P\{e_{i1}\} \\ &= \eta_q(0)(\tau - (m-1)\tau^2) + \eta_q(E[Q_j^w])(m-1)\tau^2 \\ &\quad (1 - (1-\tau)^{m-2}/2). \end{aligned} \quad (22)$$

In summary, given that the pdfs of I_i^w for MAC protocols without and with interference prevention scheme have been derived in Eq. 17 and Eq. 22 respectively, the expected value of RX_{th} for a packet transmission interval T can then be calculated as

$$RX_{th} \approx E\{\frac{\beta}{C_i}(I_i^w + \delta_w^2)\} = \frac{\beta}{C_i}(E\{I_i^w\} + E\{\delta_w^2\}). \quad (23)$$

Then, packet transmission/reception failure probability p in Eq. 5 and Eq. 6 could be derived as Eq. 16.

IV. Channel-Busy Probability Computation for MAC with Interference Prevention

For MAC protocols with carrier sensing, nodes first detect the state of the channel to determine their transmission behaviors. When the perceived signal power is larger than a value called *carrier sense threshold*, denoted as CS_{th}, the channel is regarded as busy and the packet transmission is deferred; otherwise, the channel is assumed to be idle and ready for transmission. Therefore, the channel-busy probability is also an important parameter for these MAC protocols.

Assume that a node w is sensing, and let $I'_w = \sum_{j \neq w}^{j \in Y} \chi_j Q_j^w$ represent perceived power by node w and Q_j^w represent the perceived power from node j, then the channel-busy probability P_b can be calculated as

$$P_b = P_r(\sum_{j \neq w}^{j \in Y} \chi_j Q_j^w \geq CS_{th}). \quad (24)$$

There are $m-1$ neighbor nodes within node w's two-hop perception range ($2R_s$), where $m = \left\lceil \frac{4nR_s^2}{a^2} \right\rceil$. According to our previous assumptions for efficient MAC protocols with carrier sensing, there can only exist three cases for those neighbor nodes: no node transmitting, only one node transmitting, and only two nodes transmitting concurrently. The probability of event e_{l0} that "there is no node transmitting when node w is listening," denoted by $P\{e_{l0}\}$, is $P\{e_0\}$ for $m-1$ nodes. The probability of event e_{l1} that "there is exactly one node

transmitting when node w is listening," denoted by $P\{e_{l1}\}$, is $P\{e_1\}$ for $m-1$ nodes. The probability of event e_{l2} that "there are exact two nodes transmitting concurrently when node w is listening," denoted by $P\{e_{l2}\}$, is $P\{e_2\}$ for $m-2$ nodes. Given that $P\{e_0\}$, $P\{e_1\}$ and $P\{e_2\}$ have been derived in Eq. 21, $P\{e_{l0}\}$, $P\{e_{l1}\}$, and $P\{e_{l2}\}$ can be formulated as

$$\begin{aligned} P\{e_{l0}\} &\approx 1-(m-1)\tau+(m-1)(m-2)\tau^2(1-\tau)^{m-3}/2, \\ P\{e_{l1}\} &\approx (m-1)\{\tau-(m-2)\tau^2\}, \\ P\{e_{l2}\} &\approx (m-1)(m-2)\tau^2(1-(1-\tau)^{m-3}/2). \end{aligned} \quad (25)$$

When event e_{l0} occurs, the perceived power equals zero; when event e_{l1} occurs, there is only one perceived signal caused by node j with a distance d_j to the listening node w, and the average perceived power over all the possible values of d_j, denoted as $E[Q_j^w]$, can be also calculated using Eq. 19; when event e_{l2} occurs, there are two perceived signals, and the average value of perceived power from them can be approximated as $2E[Q_j^w]$. Therefore, $f_{I'_w}(q)$ can be approximated by

$$\begin{aligned} f_{I'_w}(q) \approx\ & \eta_q(0)P\{e_{l0}\}+\eta_q(E[Q_j^w])P\{e_{l1}\} \\ & +\eta_q(2E[Q_j^w])P\{e_{l2}\}, \end{aligned} \quad (26)$$

where $\eta_q(0)$ is a Dirac pulse with $q=0$, $\eta_q(E[Q_j^w])$ is a Dirac pulse at $q=E[Q_j^w]$, and $\eta_q(2E[Q_j^w])$ is a Dirac pulse at $q=2E[Q_j^w]$.

Because the pdf of perceived power by any node w, $f_{I'_w}(q)$, has been derived in Eq. 26, Eq. 24 can be translated to

$$P_b = \int_{CS_{th}}^{\infty} f_{I'_w}(q)dq, \quad (27)$$

which is the channel busy probability g in Eq. 6

V. Throughput of MAC Protocols

In Section II, we modeled MAC protocol behaviors, and for a MAC protocol with carrier sensing, we derived its transmission probability τ as a function of packet transmission failure probability p and channel busy probability g; for a MAC protocol without carrier sensing, we derived τ as a function of p. In Section III and IV, we analyzed a realistic physical-layer behavior, and based on channel and interference conditions we derived either p or g as a function of τ.

In summary, a system of three equations can be constructed for MAC protocols with carrier sensing, and its solution provides the values for τ, p and g; for MAC protocols without carrier sensing, a system of two equations can be constructed and its solution provides the values for τ and p.

A. IEEE 802.11 DCF

Fig. 3 shows packet formats and transmission situations for IEEE 802.11 DCF. A packet includes three parts: preamble, header and data payload. Before packet transmission, a common physical-layer service access point should be achieved by sending a preamble and header, which is called physical layer convergence procedure (PLCP). In addition, the MAC and upper layers will also attach headers (H) in front of payload. After a data packet is sent out, if it is successfully received, the receiver will send an acknowledgement packet

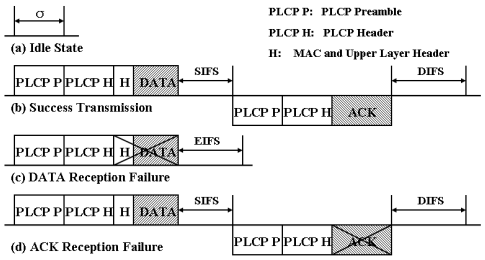

Fig. 3. Packet transmission cases

(ACK) back. However, transmission control packets, such as ACK and PLCP header, are sent with lower rate R_B, while data payloads are transmitted with higher data rate R_D.

A packet transmission may fail and sometimes there is no ongoing transmission in the channel. There are four types of packet transmissions, as shown in Fig. 3, and their durations are derived as follows. First, if no node transmits, all nodes wait for a duration $T_I=\sigma$, where σ corresponds to the idle slot interval. Secondly, if a packet is transmitted successfully, then the duration is $T_S=2t_P+\frac{H+L}{R_D}+SIFS+\frac{ACK}{R_B}+DIFS+2\xi$, where L represents the payload/data size, ACK denotes the acknowledgement packet size, ξ is the propagation delay and t_P is the duration for PLCP preamble and header. Thirdly, if a transmission fails because the receiver fails to decode the data packet, no ACK packet is issued and the receiver defers for an extended inter-frame apace interval ($EIFS=SIFS+t_P+\frac{ACK}{R_B}+DIFS$). The duration can then be expressed as $T_{FD}=t_P+\xi+\frac{H+L}{R_D}+EIFS=2t_P+\frac{H+L}{R_D}+SIFS+\frac{ACK}{R_B}+DIFS+\xi=T_S-\xi$. Fourthly, a transmission may fail because the transmitter fails to decode an ACK packet, the slot duration is the same as that of success transmission, i.e., $T_{FA}=T_S$. However, in our channel fading model we assume that an ACK packet is small enough and that fading is slow enough to guarantee the ACK packet to be received successfully if the payload/data is received successfully, i.e., we only consider transmission failure case (c) with $T_F=T_{FD}$. Particularly, the duration difference between transmission cases (c) and (d) is as small as ξ and could be neglected, which supports our assumption.

We now calculate the likelihood of the above interval durations using transmission probability τ for a node and its transmission failure probability p. For an idle slot, all the n nodes in the system keep silent. Because the silence probability of any single node is $1-\tau$, the probability of channel being idle is then $P_I=(1-\tau)^n$. The probability that at least one of the n nodes is transmitting, denoted by P_{tr}, can be formulated as $1-(1-\tau)^n$; the probability that such transmissions success, denoted as P_S, equals $\frac{n\tau(1-p)}{P_{tr}}=\frac{n\tau(1-p)}{1-(1-\tau)^n}$. Similarly, the probability that such transmissions fail, P_F, equals $\frac{n\tau p}{P_{tr}}=\frac{n\tau p}{1-(1-\tau)^n}$.

Let S represent the normalized network throughput, defined as the expected successfully transmitted payload bits per time

TABLE I
PARAMETERS USED FOR 802.11 DCF.

MAC/PHY Items	Settings
Channel access / ACK / (RTS/CTS)	(CSMA/CA) / Yes / No
Retransmission Limit / CW_{min} / CW_{max}	7 / 32 / 1024
MAC Header / ACK Size	32 / 32 (bytes)
SIFS / DIFS / Slot time / Propagation delay	10 / 50 / 20 / 1 (μsec)
Transmission power for 250 / 200 / 150 m	9.7 / 6.9 / 4.4 (dBm)
Receive Sensitivity CS_{th}	-89.0 (dBm)
Packet reception model	ERT based
Preamble synchronization / Propagation delay	192 / 5 (μsec)

unit. Then S is given by

$$S = \frac{E[L]}{E[T]} = \frac{P_{tr}P_S L}{P_I T_I + P_{tr}P_S T_S + P_{tr}P_F T_F} = \frac{Ln\tau(1-p)}{\sigma(1-\tau)^n + T_S n\tau(1-p) + T_F n\tau p}. \quad (28)$$

B. Aloha

Aloha has three packet transmission cases, idle, success and fail. Their probabilities have the same presentations as those in DCF, and the idle slot duration T_I is denoted as σ. The durations for the other transmission cases in Aloha are different with those in DCF. In Aloha, after a node sends out a packet, it waits for an acknowledgement for a fixed round-trip time slot. Hence, $T_S = T_F$ and the value can be approximated as $2 \times (t_P + \frac{H+L}{R_D} + \xi)$ where t_p represents the time needed for physical process.

VI. SIMULATIONS

A. Simulation and Modeling Setup

We consider a total of 100 nodes initially uniformly distributed over a disk area with the radius of $500m$. The Rayleigh channel fading model is employed with a data rate of 2 $Mbps$. The temperature is 290 Kelvin degrees and the noise factor is 7 dB. Every node moves following the random waypoint model at a speed of V and transmits with a radius R. Three different transmission ranges $R \in \{150, 200, 250\}m$ and four different speeds $V \in \{5, 10, 15, 20\}m/s$ are covered. Fix-size (512 bytes) data packets generated from CBR (constant bit rate) traffic flow generator with uniformly distributed sources and destinations are continuously sent out, and the rate is high enough to simulate the saturated transmission mode. Overall, a total of 12 different {radius, speed} configurations are simulated. Our analytical model is constructed with maple and matalb [16], while the discrete-event simulations are conducted in Qualnet v3.9.5 [17]. For each configuration, each simulation result is obtained from 10 random runs. Each run is conducted at a random seed with a time duration of 30 minutes.

B. Numerical Results for 802.11 DCF

Table I summarizes parameters used for 802.11 DCF. Figs. 4 and 5 show a comparison of analytical and simulation results for IEEE 802.11 DCF, where it can be observed that the analytical results derived from our proposed model provides a very good approximation to the simulation results.

The advantage of our analytical model is that it incorporates various network parameters, such as transmission range and node movement speed. Consequently, it enables the study of the impact of such parameters on protocol performance by simple computation of the equations derived in the model, rather than relying on simulations only, which can be too time consuming when many parameter values are involved. For example, as the transmission range R increases, a node can have better network view, make better determination of the channel being busy and transmitting packets, and channel signal can also become stronger to suppress the interference during packet transmission. Then the total received power increases which makes the transmission success probability increase, and finally network throughput increases, which is correctly captured by our model, as shown in Fig. 4. Mobility changes the topology of the network, and causes stronger channel fading and high link breakage probability, which increase transmission failure probability and in turn decrease network throughput. This trend is also correctly captured by our analytical model as shown in Fig. 5.

There exist small differences between the results predicted by our model and those obtained from simulation experiments. These differences are to be expected, given that we do not model the MAC protocols in great detail. Note also that we use an approximate interference model for DCF to represent the effect of other ongoing transmissions, where at most one other transmission is taken into consideration because of carrier sensing. However, when interference signals are strong enough, more interferering nodes may actually have a negative effect on the packet reception. For example, as shown in Fig. 4, when the transmission radius reaches $200m$, the channel signal of other concurrent transmissions becomes stronger and the effect of interfering nodes two hops away may not be negligible. That is, in such conditions, our model starts underestimating the negative effect of interference, and therefore starts slightly overestimating the attainable throughput. In addition, when the speed with which nodes move is not high, the channel fading effect is not strong. This implies that interference signals may be stronger than what the model assumes, and hence our model may again underestimate the negative effect of interference, i.e., overestimate the throughput a little, as shown in Fig. 5.

C. Numerical Results for ALOHA

Table II summarizes the parameters used for Aloha. We compare our analytical results with simulation results for Aloha in Figs. 6 and 7, where it can be observed that the analytical results derived from our model also provide a good approximation to the simulation results.

In Aloha, each concurrent transmission could cause an interference signal. As Fig. 6 shows, as R increases, even

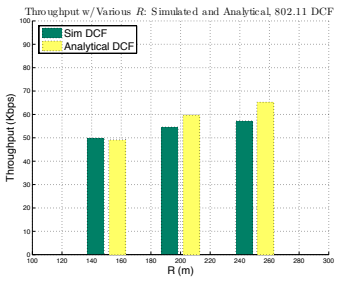

Fig. 4. DCF: Throughput vs. R.

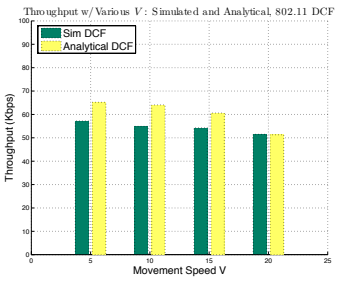

Fig. 5. DCF: Throughput vs. V.

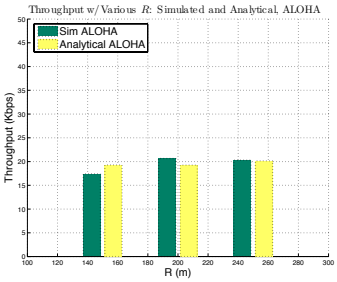

Fig. 6. ALOHA: Throughput vs. R.

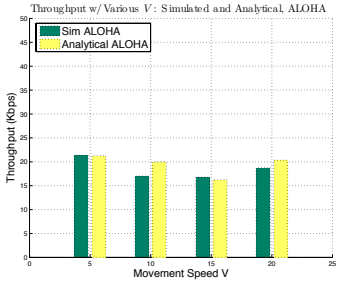

Fig. 7. ALOHA: Throughput vs. V.

TABLE II
PARAMETERS USED FOR ALOHA.

MAC/PHY Items	**Settings**
Retransmission Limit / PHY Header	5 / (192 bits)
MAC Header / ACK Size	21 / 21 (bytes)
CW / Slot time / Propagation delay	500 / 150 / 50 (μsec)
Transmission power for 250 / 200 / 150 m	16.8 / 14.0 / 11.5 (dBm)
Packet reception model / SINRT β	SINRT based / 5.0
Receive Sensitivity CS_{th}	-89.0 (dBm)

though the channel signal power becomes stronger, the number of possible interference sources may also increase. Therefore, there is no obvious network throughput increase, and when $R = 250$m the throughput even decreases slightly.

Because there is no carrier sensing in Aloha to restrict MAI, as mobility increases even the ongoing channel fading is stronger, the probability of interference nodes moving out or into the effective transmission range increases. That is, mobility causes the network and the interference effect to be more dynamic and therefore there is no clear throughput decrease trend for Aloha, which has been captured by our analytical model, as shown in Fig. 7. When node movement speed increases to a certain degree, like $20m/s$, the number of interfering sources may decrease greatly, which counteracts the stronger channel fading effect. Therefore, the throughput even starts to increase, which is shown in Fig. 7. In addition, because no carrier sensing scheme is used, the interference impact in Aloha is greater than that in DCF, which causes the network throughput of Aloha to be much smaller than that of DCF and is also captured successfully by our model.

In summary, our analytical model works very well in the modeling of the impact of the physical-layer factors on the performance of IEEE 802.11 DCF and Aloha.

VII. CONCLUSIONS

We presented an analytical two-tier Markovian model framework to capture the effect of the physical layer on the performance of MAC protocols operating in MANETs. A generic Markovian channel-state model was proposed where both noise and other concurrent transmissions (i.e., interference) are taken into account. This channel state model is embedded into the modeling of MAC protocols to capture protocol performance. Simulation results show that our analytical model works very well in representing dynamic channel-fading and interference effects on the performance of MAC protocols operating in MANETs.

In our future work, we plan to exploit advanced physical layer communication techniques into MAC protocol design and analyze how and how much performance improvement they can bring.

REFERENCES

[1] G. Bianchi, "Performance analysis of the ieee 802.11 distributed coordinationfunction," *IEEE Journal on Selected Areas in Communications*, vol. 18, pp. 535–547, March 2000.

[2] R. T. B. Ma, V. Misra, and D. Rubenstein, "Modeling and analysis of generalized slotted-aloha mac protocols in cooperative, competitive and adversarial environments," in *IEEE International Conference on Distributed Computing Systems*, Portugal, July 2006, pp. 62–69.

[3] T. S. Rappaport, *Wireless communications, principles & practice*, 2nd ed. Upper Saddle River, NJ: Prentic Hall PTR, 2001.

[4] F. Belloni, "Fading models," in *POSTGRADUATE COURSE IN RADIO COMMUNICATIONS*, Autumn 2004, pp. 1–4.

[5] M. M. Carvalho and J. J. Garcia-Luna-Aceves, "Modeling wireless ad hoc networks with directional antennas," in *IEEE Infocom*, Barcelona, Spain, Apr. 2006, pp. 13–26.

[6] Y. Zheng, K. Lu, and D. Fang, "Performance analysis of ieee 802.11 dcf in imperfect channels," *IEEE Transactions on Vehicular Technology*, vol. 55, pp. 1648–1656, September 2006.

[7] P. Pham, S. Perreau, and A. Jayasuriya, "New cross-layer design approach to ad hoc networks under rayleigh fading," *IEEE Journal on Selected Areas in Communications*, vol. 23, pp. 28–39, Jan. 2005.

[8] P. P. Pham, "Comprehensive analysis of the ieee 802.11," *Mobile Networks and Applications*, vol. 10, pp. 691–703, October 2005.

[9] N. Abramson, "The aloha systemcanother alternative for computer communications," in *AFIPS Conference Proceedings*, vol. 36, May 1970, pp. 295–298.

[10] *Wireless LAN medium access control (MAC) and physical layer (PHY) specifications*, Revision of ieee std 802.11-1999 ed. New York, USA: ISO/IEC 8855-1331, June 2007.

[11] L. Roberts, "Aloha packet system with and without slots and capture," in *ACM SIGCOMM Computer Communication Review*, vol. 5, April 1975, pp. 28–42.

[12] M. Takai, J. Martin, and R. Bagrodia, "Effects of wireless physical layer modeling in mobile ad hoc networks," in *International Symposium on Mobile Ad Hoc Networking & Computing*, Long Beach, CA, USA, Oct. 2001, pp. 87–94.

[13] C. Bettstetter, "Topology properties of ad hoc networks with random waypoint mobility," in *ACM SIGMOBILE Mobile Computing and Communications Review*, vol. 7, July 2003, pp. 50–52.

[14] F. Babich and G. Lombardi, "A markov model for the mobile propagation channel," *IEEE Transactions on Vehicular Technology*, vol. 49, pp. 63–73, Jan. 2000.

[15] F. Babich, O. E. Kelly, and G. Lombardi, "Generalized markov modeling for flat fading," *IEEE Transactions on Communications*, vol. 48, pp. 547–551, April 2000.

[16] *The MathWorks*, v. 7.0. ed.

[17] *Scalable Network Technologies*, Qualnet simulator v. 3.9.5 ed.